Molecular dynamics simulations of some amorphous and crystalline photonic materials

Pradeep P. Phule,[a] Pierre A. Deymier, and Subhash H. Risbud[b]
Department of Materials Science and Engineering, University of Arizona, Tucson, Arizona 85721

(Received 17 May 1989; accepted 2 February 1990)

Constant pressure molecular dynamics (MD) simulations have been used to simulate amorphous and crystalline forms of $BaTiO_3$ and TiO_2. Simulation results for pure $BaTiO_3$ and TiO_2 glasses show fourfold titanium coordination with a Ti–O bond distance of 1.8 Å, consistent with experimental evidence for the structure of titania doped glasses for all optical switching and ultra low expansivity (ULE) TiO_2–SiO_2 glasses. Radial distribution function data for crystalline, liquid, and amorphous forms of $BaTiO_3$ were also obtained. The displacement polarization and its contribution to susceptibilities have been calculated by application of an electric field to the simulation cell. The calculated ionic dielectric constants (K_i) for simulated NaCl (crystal), TiO_2 glass, and TiO_2 (crystal) were 3.34, 5.96, and 19.4 as compared to the experimental values of ≈3.34, 3–10, and 78, respectively. The calculated cubic nonlinear susceptibility (ξ_3) values for NaCl (crystal), TiO_2 (glass), and TiO_2 (crystal) were, respectively, 0.194, 2.175, and 4.68 ($\times 10^{-18}\,m^2\,V^{-2}$). The increase in ξ_3 values is consistent with experimentally observed trends of the linear refractive indices. Improved agreement between experimental and calculated values of susceptibilities and dielectric constant was obtained for materials with higher ionicity.

I. INTRODUCTION

Development of new materials for photonic applications is the theme of many current activities in materials science and technology. Barium titanate ($BaTiO_3$) with a large electro-optic coeffficient[1] and TiO_2 containing sodium silicate glasses[2] with relatively high nonlinear refractive indices ($n_2 \approx 1$–$10 \times 10^{-19}\,m^2/W$) are considered to be some of the promising photonic materials. While experimentation continues to be the major source for obtaining information regarding the structure and properties of these and other materials, recent advances in development of atomistic computational procedures such as molecular dynamics (MD) may prove valuable in circumstances in which the appropriate experiments are difficult to perform. MD also allows structural insights that may explain experimental observations and provide predictive tools for the properties of these emerging materials.

Experimental difficulties exist in preparation of large, defect-free, optical quality $BaTiO_3$ single crystals, although amorphous $BaTiO_3$ gels and crystalline powders have been prepared[3–5]; however, it is difficult to prepare pure $BaTiO_3$ glasses in large quantities.[6] In the case of TiO_2 containing glasses, relatively large nonlinear refractive indices are observed and are believed to be due to the presence of tetrahedrally coordinated titanium ions.[2] This argument has also been used to explain the ultra low expansivity of the TiO_2–SiO_2 glasses.[7] In sputtered amorphous films the coordination number of titanium may be 4 or 6, depending upon the type and concentration of other cations.[8]

With a view to developing a better understanding of the structure-property relationships for $BaTiO_3$ and titania containing glasses, the MD technique was utilized in the present work to simulate crystalline and amorphous forms of $BaTiO_3$ and TiO_2. A rigid ion potential model was used in all the MD simulations which were also performed onNaCl, a highly ionic material, to provide an internal check for the accuracy of the model.

II. MOLECULAR DYNAMICS SIMULATIONS TECHNIQUE

Molecular dynamics (MD) simulations represent a powerful tool for deriving the local structure of a variety of amorphous and crystalline materials. MD essentially consists of solving the classical equations of motion of an assembly of particles interacting through realistic interatomic potentials. The solution of these equations provides important quantitative information regarding the structure of materials and thus predict properties.

The time resolution of MD technique is on the order of 10^{-15} s, which makes it particularly attractive for a study of optical properties in the IR region. We

[a]Now with the Department of Materials Science and Engineering, 848 Benedum Hall, University of Pittsburgh, Pittsburgh, Pennsylvania 15261.
[b]Now with the Department of Mechanical, Aeronautical, and Materials Engineering, University of California, Davis, California 95616.

have used a realistic MD formalism allowing for the simulation of ionic systems in periodic cells with fluctuating shape and volume.[9]

In this constant stress MD formulation, three variable vectors, $\mathbf{e}_1$, $\mathbf{e}_2$, and $\mathbf{e}_3$, forming 3×3 matrix H, describe the planar boundaries of the simulation cell. The volume of the simulation cell is given by $\omega = \mathbf{e}_1 \cdot (\mathbf{e}_2 \times \mathbf{e}_3)$. The position r_i in a fixed Cartesian coordinate system may be expressed in variable coordinate system as $s_i = H^{-1} r_i$. The edges of the simulation cell are driven by the imbalance between an externally applied stress σ and the internal stress vector. The Hamiltonian governing the equations of motion of the system under a constant stress σ is written as

$$H = \sum_i \left(\frac{1}{2} m_i v_i^2\right) + \phi_{ij}(r_{ij}) + \frac{1}{2} W \, Tr(\hat{H}^T \hat{H}) + Tr\{\sigma\epsilon\}\,\omega_0$$

where $\hat{H} = dH/dt$. H^T and $Tr\,H$ are the trace and transpose of the matrix H, respectively. The total energy is the sum of the kinetic and potential energies of the set of particles, the kinetic energy of the borders of the simulation cell to which is artificially assigned a mass W, and the elastic energy, for which ω_0 is the volume of the reference system used to measure a small strain ϵ. Average quantities calculated along the trajectories of the above Hamiltonian are independent of W, while the dynamical properties are not. To maintain a constant temperature, particle momenta are rescaled.

For computational convenience, it is usually assumed in MD that the interaction between the ions in the system is central pair-wise additive. We have used a Born-Mayer-Huggins type potential:

$$\phi_{ij}(r) = q_i q_j e^2/r + A_{ij} \exp[-r/\sigma_{ij}] - C_{ij} r^{-6}$$

where r is the interionic distance, q_i is the ionic charge (-2, $+2$, and $+4$ for oxygen, barium, and titanium, respectively) for species i, and C_{ij} is a coefficient in the short-range van der Waals attraction term. The exponentially decaying repulsive term is composed of two parameters, A_{ij} and σ_{ij}.

We have used an extension of the constant stress molecular dynamics formalism of Parinello and Rahman[10] to simulate assemblies of particles interacting through the long-range Coulombic potentials. The simulation involves the summation of the Coulombic energy potential and forces among all pairs. In order to expedite the convergence of the potential summation series, the Ewald summation method was incorporated in the MD algorithm. The potential parameters for $BaTiO_3$ used here have been used by Lewis and Catlow[11] in their defect energy calculations. We used the same Ti–O, O–O parameters for TiO_2 simulations. NaCl was simulated using the potential reported by Sangster and Atwood.[12]

III. MOLECULAR DYNAMICS SIMULATION OF NONLINEAR POLARIZATION EFFECTS

The electric polarization P (electric dipole moment per unit volume) of a dielectric medium subjected to an electric field E, is given by the relationship:

$$P = \epsilon_0 \, \xi(E) \cdot E$$

where $\xi(E)$ is the usual linear susceptibility tensor. Expanding $\xi(E)$ as a power series in E, this relationship may be rewritten as

$$P = \epsilon_0 \{\xi_1 \cdot E + \xi_2 \cdot E \cdot E + \xi_3 \cdot E \cdot E \cdot E + \ldots\}$$

where ξ_1 is the usual linear susceptibility tensor and ξ_2 and ξ_3 are the quadratic and cubic nonlinear susceptibility tensors, respectively. When an electromagnetic wave is incident upon a medium, ξ_1 is responsible for the linear optical properties such as reflection and refraction; ξ_2 gives rise to nonlinear phenomena of second harmonic generation as well as sum and difference frequency mixing, optical rectification, linear electro-optic effect, and parametric generation; ξ_3 is responsible for third harmonic generation, quadratic electro-optic effect, two phonon absorption and stimulated Raman, and Brillouin and Rayleigh scattering.

From the microscopic point of view, the linear susceptibility arises from the response of the electrons as well as the ions, to the electromagnetic wave. Electrons will respond to radiations with frequencies below those of phonons, and both contributions have to be considered. If the frequency is higher than that of the ionic vibrations, the ions cannot follow the variations of the electric field of the radiation and the susceptibility is essentially due to the electrons. In general, the susceptibility of a medium will be written as $\xi = \xi_i + \xi_e$, where ξ_i and ξ_e denote the ionic and electronic contributions to the susceptibility, respectively. Nonlinearity in the electrons/ions responses to the electric field contributes to the quadratic and cubic susceptibilities as well.

The equations of motion of the ions and borders of the simulation cell have been modified to include interaction with an external electric field $E(t)$. The Hamiltonian of the perturbed system is:

$$H = H_0 - M \cdot E(t)$$

where H_0 is the Hamiltonian of the unperturbed system and M, the dipole moment. The total dipole moment of the system of N charged particles with charges q_i is defined as $M = \Sigma\, q_i \cdot r_i$. The applied electric field is superimposed onto the internal microscopic field of the simulation cell. The atoms in the simulation cell experience the sum of local and applied electric fields.

With a view to studying the potential of the MD technique for computation of linear and nonlinear optical properties, the ionic contribution to the differential polarization $\Delta P = (P_{\text{perturbed system}} - P_{\text{unperturbed system}})$ was calculated as a function of the magnitude of an external uniform static electric field E. The data obtained from simulations were fitted to a polynomial, from which the values of ξ coefficients were calculated.

The ionic dielectric constant was calculated from the linear susceptibility value using the following equation:

$$K_i\,(\text{MD}) = 1 + \xi_i$$

Since the simulations account only for ionic polarizability, K_i (MD) was compared to the ionic dielectric constant (K_i) obtained as follows:

$$K_i = K - K_e$$

$$K_e = n^2$$

where K, K_e, and n stand for experimental dielectric constant, electronic dielectric constant, and measured linear refractive index, respectively.

For $BaTiO_3$, the MD algorithm time step was 1.073×10^{-14} s and the pressure $P = 1$ atm. The total number of ions in the MD cell was 135, consisting of 27Ba, 27Ti, and 81O ions. Single crystal $BaTiO_3$ was simulated at 298 K. Structure of pure $BaTiO_3$ glass was studied by ultrafast cooling of $BaTiO_3$ liquid, simulated at 3000 K. Similarly, crystalline (rutile) and amorphous forms of TiO_2 were simulated using a simulation cell containing 72Ti and 144O ions. The time step was 1.073×10^{-14} s. The single crystal was simulated at 298 K. Pure TiO_2 glass was simulated by freezing the liquid simulated at 3000 K. Sodium chloride single crystal was simulated at 298 K, with 108Na and 108Cl ions in the simulation cell. The time step used in NaCl simulations was 3.215×10^{-15} s. In all cases, the simulations lasted at least 2000 integration time steps and up to 3000 time steps when larger electric fields were applied. The first 200 steps were discarded in the calculation of time averages.

IV. RESULTS AND DISCUSSION

A. Structural simulations of crystalline and amorphous $BaTiO_3$

Based on the potential parameters presented in Table I, a barium titanate single crystal was simulated at 298 K. The interionic distances and volume calculated using the simulation data match well with the experimental data (Table II). The coordination numbers of Ti and Ba were computed from simulation data with a cut-off radius to the first minimum and second minimum of the (+ −) partial radial distribution function, respectively. The partial radial distribution functions

TABLE I. Potential parameters for $BaTiO_3$.

	A_{ij}, eV	σ_{ij}, Å	C_{ij}, eV (Å)^6
Ba–O	1214.4	0.3522	8.0
Ti–O	877.2	0.3800	9.0
O–O	22764.0	0.1490	43.0

TABLE II. Comparison of experimental interionic distances and ion coordination of $BaTiO_3$ with simulated single crystal and amorphous $BaTiO_3$.

	Interatomic distance (Å)		
Ion-Pair	Experimental crystal	Simulated crystal	Simulated glass
Ti–O	2.01	2.00	1.80
Ba–O	2.85	2.85	2.30
Ba–Ti	3.49	3.49	3.50
O–O	2.85	2.85	2.85
	Cation coordination number		
Titanium	6	6	4
Barium	12	12	8

(RDF) of crystalline $BaTiO_3$ obtained from the simulation data are presented in Fig. 1. These data confirm the experimentally observed octahedral coordination of Ti with a Ti–O bond distance of 2.01 Å. Similarly, the

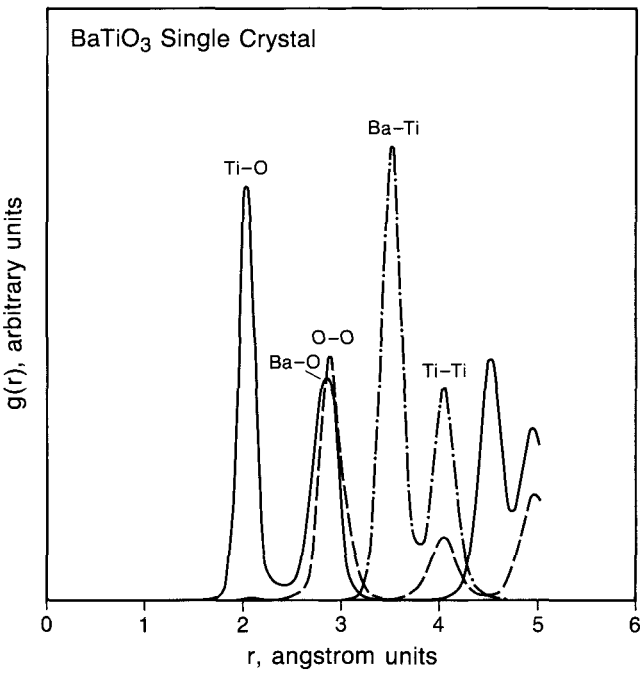

FIG. 1. Partial radial distribution of simulated $BaTiO_3$ crystal.

Ba–O distance (2.85 Å) and coordination number (12) computed from the simulations also exhibit an excellent match with the experimentally observed structure of $BaTiO_3$.

Figure 2 shows the relatively broad peaks in the radial distribution function of pure $BaTiO_3$ liquid. Barium titanate glass was obtained by rapidly quenching this liquid to room temperature (cooling rate $\approx 10^{19}$ °C/s). The radial distribution function data of the thus obtained glass are presented in Fig. 3. The interionic distances and ion coordinations for $BaTiO_3$ glass are presented in Table II. Analysis of the simulation data for pure $BaTiO_3$ glass revealed strikingly different distance and coordination number for Ba and Ti. The Ti–O distance of 1.8 Å and calculated coordination number imply that the Ti in these simulated glasses exists predominantly in a fourfold coordination. Similar results obtained for simulations of pure TiO_2 crystal and glass are summarized in Table III.

This observation is important since the local oxygen environment about the Ti cation can affect its optical properties. The change in the Ti–O distance from 2.01 to 1.8 Å has also been believed to be responsible for the ultra low expansivity and relatively large ξ_3 of the titania containing silica glasses. In these glasses as well as in sputtered films Ti has also been believed to be in tetrahedral coordination in Ref. 8. In compounds such as Ba_2TiO_4, an intermediate phase occurring in the conventional synthesis of $BaTiO_3$[13] and $TiCl_4$ have also been known to show Ti in fourfold coordination.

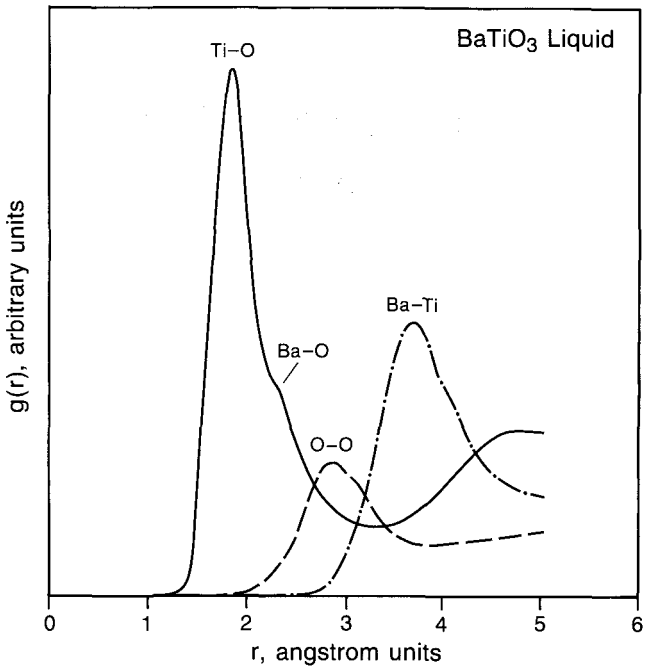

FIG. 2. Partial radial distribution of simulated liquid $BaTiO_3$ (3000 K).

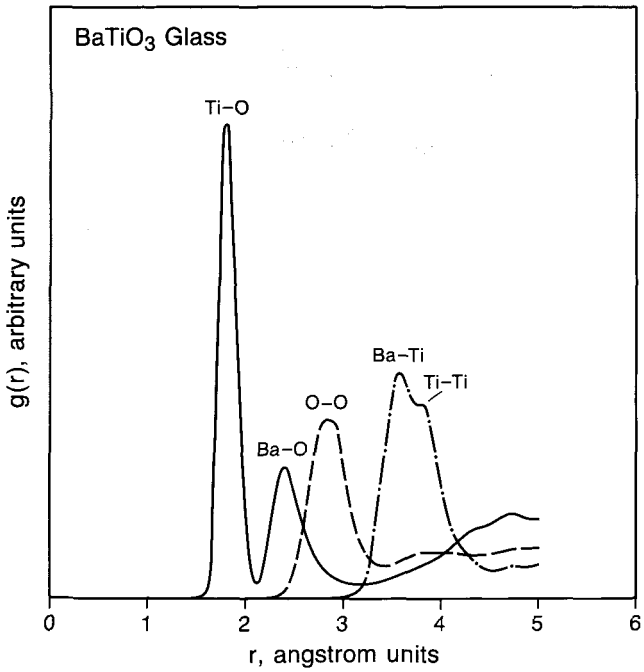

FIG. 3. Partial radial distribution of simulated pure $BaTiO_3$ glass.

Recently, Rosenthal and Garofalini[14] have also used constant volume MD simulations to demonstrate the change in Ti coordination in the SiO_2–TiO_2 system as a function of the glass composition. It would also be a useful contribution to investigate experimentally the local structure of amorphous materials in the SiO_2–TiO_2 system containing up to 90% TiO_2.[15]

A note of caution about the interpretation of the MD simulation results is appropriate at this juncture. The simulation results predict structure of amorphous materials obtained under conditions of formation (e.g., cooling rate $\approx 10^{19}$ °C/s, no impurities, etc.) that are practically unattainable by experimental techniques. This is both an advantage and a problem, since although one can generate and study novel materials using a computer, care has to be exercised in interpretation and correlation of the simulation results to the experimental data. The results of these simula-

TABLE III. Comparison of simulated and experimental TiO_2 structures.

Cell parameters	
Experimental crystal	Simulated crystal
a = 4.593 Å	a = 4.639 Å
c = 2.959 Å	c = 3.250 Å
Titanium coordination	
Crystal (experimental):	Octahedral
Simulated crystal:	Octahedral
Simulated glass:	Tetrahedral

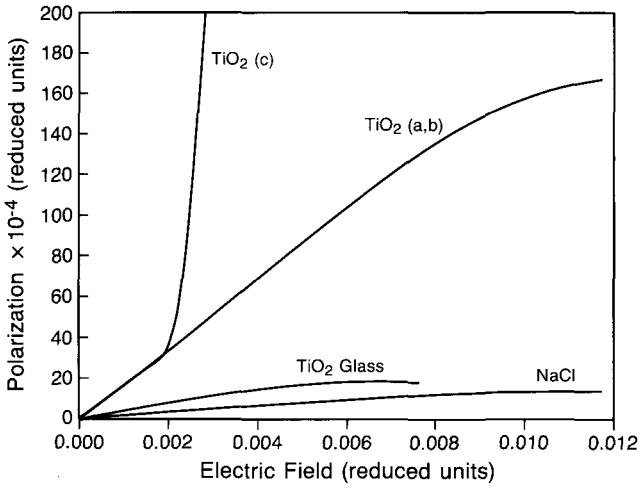

FIG. 4. Polarization ($\Delta P^* \times 10^4$) of simulated materials as a function of applied electric field (E^*).

tions suggest that titanium may exist in a fourfold coordination. The TiO_2-containing glasses, for photonic applications,[2] have complex compositions and the effects of other cations on the coordination of titanium and the possibility of phase separation at a very fine scale during processing must also be carefully considered and evaluated.

B. Optical and dielectric properties

As explained earlier, the original MD algorithm was modified to apply a uniform electric field over the entire simulation cell. Figure 4 shows the results of the calculated displacement polarization (ΔP) versus applied electric field (E) for NaCl and TiO_2 (glass and crystal). The data for differential polarization as a function electric field were fitted to a polynomial and the ξ_1, ξ_2, and ξ_3 were calculated (Table IV), after appropriate conversions of the reduced units to MKSI units [$E(\mathrm{Vm}^{-1}) = E^* \cdot 1.44 \times 10^{11}$, $P\ (\mathrm{Coul\ m}^{-2}) = 16.02 \cdot P^*$].

Results of sodium chloride simulations showed that the calculated ionic dielectric constant [K_i (MD) = 3.34] matches very well the experimentally observed value (3.34) (Table V). Since a rigid ion potential model is used in the MD simulations, the agreement between experimental and calculated values is very good for materials with high ionicity. Note that the ξ_2 for NaCl is small, but not zero (Table IV). This is due to the distortion of the originally centric crystal by the application of relatively high electric fields.

For crystalline TiO_2, when the electric field is applied in the a or b direction, the structure is stable and nonlinear reponse is observed at high fields ($E = 1.00 \times 10^9$ V/m, $E^* = 0.007$, Fig. 4). When the electric field is applied in the c direction, the structure is unstable at relatively smaller fields ($E = 3.6 \times 10^8$ V/m, $E^* = 0.0025$, Fig. 4) and a structural breakdown occurs,

TABLE IV. Calculated ξ coefficients for simulated TiO_2 and NaCl.

	NaCl crystal	TiO_2 glass	TiO_2 crystal
ξ_1	2.337	4.960	18.398
$\xi_2 \times 10^{-10}$ m^1 V^{-1}	1.396	6.332	7.350
$\xi_3 \times 10^{-18}$ m^2 V^{-2}	0.194	2.175	4.666
$\xi_2/\xi_1 \times 10^{-10}$	0.597	1.276	0.399
$\xi_3/\xi_1 \times 10^{-18}$	0.083	0.438	0.253

TABLE V. Comparison of calculated and experimental values of dielectric constant for TiO_2 and NaCl.

	NaCl crystal	TiO_2 glass	TiO_2 crystal
K, experimental dielectric constant, 10^6 Hz[a]	5.90	5–10[b]	85.8 (a, b) 170.0 (c)
n, experimental linear refractive index	1.60	1.5[b]	2.76
Electronic dielectric constant K_e ($= n^2$)	2.56	2.25[b]	7.61
Experimental ionic dielectric constant $K_i = K - K_e$	3.34	2.75–7.75[b]	78.19 (a, b) 162.38 (c)
K_i (MD), calculated ionic dielectric constant (from MD simulations)	3.34	5.96	19.4 (a, b) 19.4 (c)

[a]From *Introduction to Ceramics*, by W. D. Kingery, H. K. Bowen, and D. R. Uhlmann (1976), p. 933.
[b]Typical values for silicate glasses.

which is seen by a rapid increase in the calculated ionic polarization.

The experimental ionic dielectric constant for TiO_2 is much higher ($\approx$78) than what is predicted by MD calculations ($\approx$19). This may be due to the inherent limitation of rigid ion potential models to simulate materials such as TiO_2, with only $\approx$60% ionic character. The Ti–O bond is too rigid with the ionic model, resulting in a breakdown in the c direction, for relatively small ionic displacements. Furthermore, the MD calculations also predict similar ionic dielectric constants (19.4) for TiO_2 crystal in (a, b) and c (prior to breakdown) directions as compared to the experimental values of 78.19 (a, b) and 162.38 (c) (Table V). Contribution of electronic origin are known to be dominating in oxides as compared to halides.[16] The rigid ion model used in these MD simulations assumes existence of a stable O^{-2} ion. It is known that for such oxides as TiO_2 and $BaTiO_3$, the oxygen may exist as O^{-1} and an electron (e^-) stabilized by the Madelung potential.

For pure titania glass, the polarization (in any direction) is less than that for crystalline TiO_2 since the distortion of the tighter TiO_4 polyhedra is more difficult. This observation is consistent with the low ther-

mal expansivity of the titania-silica glasses in which the titanium is believed to be in tetrahedral coordination. The calculated ionic dielectric constant value (≈6) matches reasonably well with the ionic dielectric constant for silicate glasses (≈3–8) (Table V). These results suggest that the ionic polarization contributions are more important for simulated TiO_2 glass as compared to the crystal. We are currently developing a more sophisticated dynamical model which accounts for the electronic polarizability effects.

V. SUMMARY AND CONCLUSIONS

The technique of MD has been applied to several materials of interest in photonic applications. The rigid ion potential model has been used to successfully simulate structures of crystalline and amorphous $BaTiO_3$ and TiO_2. The structure of simulated $BaTiO_3$ crystal is in very good agreement with the experimental data. The calculated coordination numbers for the simulated pure TiO_2 and $BaTiO_3$ glasses indicate that the Ti is predominantly in a tetrahedral coordination in these materials. This is in accordance with the experimentally observed coordination of Ti in titania doped glasses for high-speed optical switching,[2] low expansivity titania-silica glasses, and amorphous thin films containing titanium.

The MD algorithm has been further modified to allow for the application of an electric field. The displacement polarization–electric field curves calculated using simulation data have been used to derive the contributions of ionic polarization to the linear and nonlinear susceptibilities of NaCl (crystal) and TiO_2 (rutile crystal and glass). Using these data, we have observed nonlinearity, due to the ionic displacement polarizability in NaCl and TiO_2 (rutile crystal and glass). The electric fields at which the simulated materials exhibit nonlinear effects are higher than those required for electrical breakdown of most ceramics. The magnitude of calculated nonlinear coefficients (Table IV) scales with the experimental values of linear refractive indices (Table V), consistent with the generally accepted rule of thumb for NLO materials. The refractive index and nonlinear coefficients for TiO_2 crystal are higher than those for TiO_2 glass. However, glasses are one of the leading candidates for NLO applications because of the ease of production of optical quality materials. The calculated and experimental linear susceptibility and dielectric constant values show increasing agreement for materials with high ionicity.

Future research efforts directed toward studying the extent and effects of electronic contributions on the nonlinear optical properties of TiO_2, $BaTiO_3$, and inorganic glasses will be valuable. Simulations of glasses with more complex compositions coupled with synthesis and characterization of novel glasses by a variety of experimental techniques should lead to reliable structure-property models for novel optical and photonic materials.

ACKNOWLEDGMENTS

This work is based on part of P. P. Phule's Ph. D. dissertation at the University of Arizona. We are grateful to the College of Engineering and Mines for generous allocation of computer time.

REFERENCES

[1]A. M. Glass, Mater. Res. Bull. **8**, 16 (1988).
[2]D. M. Krol and E. M. Vogel, paper 3-NLO-88P, presented at the 41st Pacific Coast Regional Meeting of the American Ceramic Society, San Francisco, CA, October 23–26, 1988.
[3]P. P. Phule and S. H. Risbud, Adv. Ceram. Mater. **3**, 183 (1988).
[4]P. P. Phule and S. H. Risbud, *Better Ceramics Through Chemistry*, edited by C. J. Brinker, D. R. Clark, and D. R. Ulrich (Materials Research Society, Pittsburgh, PA, 1988), Vol. 3, p. 275.
[5]P. P. Phule and S. H. Risbud, Mater. Sci. and Engg. **B3**, 241 (1989).
[6]D. R. Ulrich, Ph. D. Thesis, State University, Rutgers, from H. Rawson (Academic Press, New York, 1967), p. 202.
[7]P. C. Schultz and H.T. Smyth, in *Amorphous Materials* (Wiley-Interscience, London, 1972), p. 453.
[8]N. Soga and T. Hanada, Diffusion and Defect Data **53-54**, 265 (1987).
[9]M. Parinello and A. Rahman, J. Appl. Phys. **52**, 7182 (1981).
[10]M. Parinello and A. Rahman, in *The Physics of Superionic Conductors and Electrode Materials,* NATO-ASI, Odense, edited by J. Perran (Plenum, New York, 1980).
[11]G.V. Lewis and C. R. A. Catlow, Phys. Chem. Solids **47**, 89 (1986).
[12]M. J. L. Sangster and R. M. Atwood, J. Phys. C **111**, 1541 (1978).
[13]P. P. Phule and S. H. Risbud, J. Mater. Sci. (in press).
[14]A. B. Rosenthal and S. H. Garofalini, J. Non-Cryst. Solids **107**, 65 (1988).
[15]H. Morikawa, T. Osuka, F. Marumo, A. Yasumori, M. Yamane, and M. Momura, J. Non-Cryst. Solids **82**, 97 (1986).
[16]M. J. Weber, D. Milam, and W. L. Smith, Optical Engineering **17**, 463 (1978).